LA-UR-97-984

CONF-970302--3

Title: Interplay Between Electronic Transport and Magnetic Order in Ferromagnetic Magnetic Manganite Thin Films

Author(s):
M.F. Hundley
J.J. Neumeier
R.H. Heffner
Q.X. Jia
X.D. Wu
J.D. Thompson

Submitted to:
Materials Research Society
Spring Meeting
San Francisco, CA
March 31-April 4, 1997

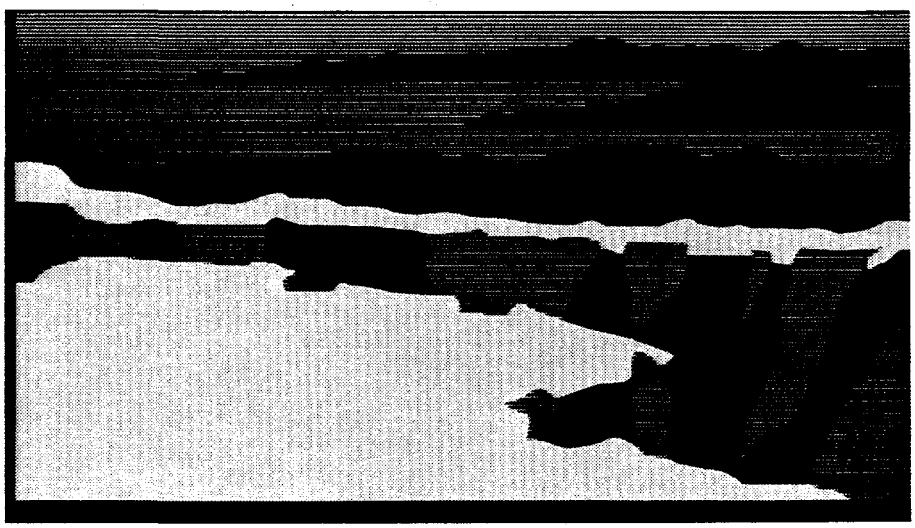

Los Alamos
NATIONAL LABORATORY

Form No. 836 R5
ST 2629 10/91

DISCLAIMER

Interplay Between Electronic Transport and Magnetic Order in Ferromagnetic Magnetic Manganite Thin Films

M.F. Hundley, J.J. Neumeier*, R.H. Heffner, Q.X. Jia, X.D. Wu, and J.D. Thompson
Los Alamos National Laboratory, Los Alamos, NM 87545

ABSTRACT

The transition metal oxides $La_{1-x}A_xMnO_3$ (A = Ba, Ca, or Sr) order ferromagnetically with Curie temperatures ranging from as low as 50 K to well above room temperature. Magnetic order in these compounds results in a concomitant metal-insulator transition. The feature displayed by the manganites that is most important technologically is the extremely large negative magnetoresistance that achieves its largest values near the magnetic ordering temperature. Qualitatively, this colossal magnetoresistance (CMR) phenomenon involves the suppression of the relatively sharp maximum in the resistivity that is centered at T_C. When considered collectively, the anomalous temperature-dependent transport properties, the CMR effect, and the magnetically ordered ground state indicate that a novel interplay between magnetism and electronic transport occurs in the manganites. General features of the magnetic-field and temperature-dependent electrical resistivity and magnetization as displayed by PLD-grown thin films are examined. Particular emphasis is placed on what these measurements tell us about the conduction process both above and below the magnetic ordering temperature.

INTRODUCTION

The electronic transport and magnetic properties of the doped ferromagnetic (FM) semiconductors $La_{1-x}A_xMnO_{3+\delta}$ (A = Ba, Ca, or Sr) were first examined many years ago [1,2]. Undoped $LaMnO_3$ is an insulating super-exchange antiferromagnet (AFM), while divalent substitution for La^{3+} leads to a mixed $Mn^{3+/4+}$ nominal valence, a FM ground state intimately associated with a metal-insulator (MI) transition at $T_{MI} = T_C$, and the colossal magnetoresistance (CMR) [3] effect. The unusual temperature and magnetic field dependent resistivity exhibited by these compounds reflects a novel interplay between magnetism and electronic transport that does not occur in conventional metals, ferromagnets, or semiconductors. The concept of Double Exchange (DE) was proposed to account qualitatively for the close interplay between magnetic order and electronic transport in these compounds [4]. The recent rediscovery of the CMR effect [5,6] has lead to renewed interest in these compounds with an emphasis on moving beyond the basic notions of DE in order to uncover the physical mechanisms involved in the CMR effect. The emerging theoretical picture is that DE alone cannot account for the physical behavior of the CMR system at other than a very crude level [7]. Instead, it may be that the CMR effect stems from an interplay between magnetic exchange and a strong electron-phonon interaction that occurs due to the Jahn-Teller (JT) active octahedrally coordinated $3d^4$ ions present in these materials [7]. In this scenario [8] the interplay between the spin, charge, and lattice degrees of freedom leads to localized small-polaron quasiparticles in the paramagnetic state, while long-range order delocalizes the carriers, leading to metallic-like large polaron transport below T_C. In support of this picture, experimental evidence [9-11] indicates that de-localized polaron-like effects persist below T_C.

In this paper we examine three aspects of electronic transport and magnetism in manganite thin films. First, we examine the general temperature and magnetic field dependence exhibited by PLD-grown thin films and compare them to the properties displayed by polycrystalline bulk

samples. Second, to determine how resistivity and magnetic order are interrelated in these compounds we present the results of careful $\rho(H,T)$ and $M(H,T)$ measurements performed on high-quality $La_{0.7}Ca_{0.3}MnO_3$ thin films with the goal of determining the functional correlation between these quantities. Lastly, to determine the dependence of the CMR effect on T_C, we examine the temperate and H-field dependent resistivities of a series of $La_{0.7}A_{0.3}MnO_{3+\delta}$ thin films with T_C's ranging from 150 to 350 K. We will show that the CMR effect is a strong function of sample T_C. Throughout this paper, the correlations and dependencies exhibited by the manganites will be employed to make important insights into the nature of the mechanisms responsible for the CMR effect.

EXPERIMENTAL

Highly oriented 1000 Å thick films were deposited on (100) $LaAlO_3$ substrates with pulsed-laser deposition (PLD) from composite targets of $La_{0.7}A_{0.3}MnO_3$ (A = Ba, Ca, or Sr). The PLD process which was carried out in a 200 mTorr oxygen atmosphere. In agreement with previous work [6,12,13] a post-anneal is critical in order to obtain high-quality films. Our films were therefore annealed in flowing oxygen at 950 °C for ten hours. This process raises T_C, drops ρ by two to three orders of magnitude, and sharpens the magnetic signature of the FM transition. Rutherford back-scattering measurements indicate that the annealing process increases the oxygenation by 1% to 3%. Scanning-tunneling and atomic-force microscopy reveal that the annealing process produces a ten-fold increase in grain size (to roughly 500 nm). The post-annealed films were patterned using conventional photolithography and ion milling into a six-terminal configuration suitable for ρ and Hall effect (R_H) measurements. Electrical contacts were made with a silver conductive paint. Four-probe R_H and ρ measurements were performed using dc currents ranging from 1 nA to 1 μA. The temperature was controlled with a capacitance thermometer during field sweeps (critical when examining samples with a large $d\rho/dT$), while the zero-field temperature was determined with a carbon-glass temperature sensor. All magnetoresistance (MR) data presented here are transverse MR (current in the film plane, H applied perpendicularly to the film plane); the MR is defined as $\Delta\rho/\rho_o \equiv (\rho(H)-\rho(H=0))/\rho(H=0)$. Magnetization measurements were performed with the same sample orientation using a Quantum Design SQUID magnetometer.

RESULTS

$\rho(H,T)$ in CMR films

The temperature-dependent zero-field resistivity and 2 kOe magnetization of a $La_{0.7}Ca_{0.3}MnO_3$ film grown with a substrate temperature T_s of 600 C are shown in Fig. 1. The H = 0 and H = 50 kOe resistivities for this same film are depicted in Fig. 2. Arrott plots (H/M vs. M^2) indicate that $T_C = 250\ K \pm 5\ K$ for this specimen; this is precisely the temperature where the resistivity and MR are largest. The resistivity displays Arrhenius behavior above T_C with an activation energy E_a = 0.1 eV (1160 K). Hall measurements at 300 K give a carrier concentration $n \approx 0.3$ carriers per formula unit, a drift mobility $\mu_D \approx 0.02\ cm^2/V\text{-sec}$, and a mean-free path smaller than a lattice constant. The short mean-free path and very small mobility suggest that conduction proceeds via nearest-neighbor adiabatic small polaron hopping above T_C rather then by semiconducting transport. Recent thermopower and Hall effect measurements confirm this view [14,15]. Below T_C, ρ drops sharply, reaching values characteristic of a dirty metal below 30 K (~ 140 μΩ-cm). A

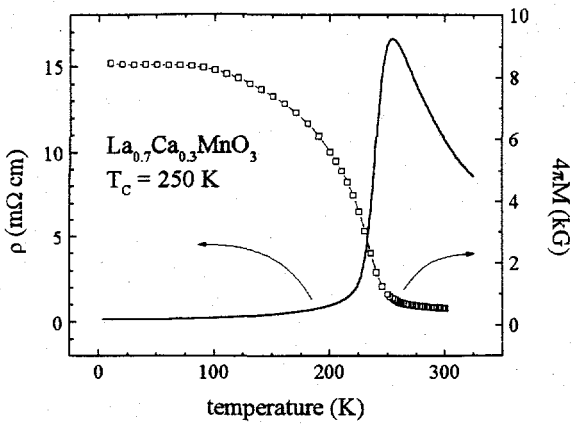

Fig. 1. ρ(T) and M(T) for a film with T_C = 250 K.

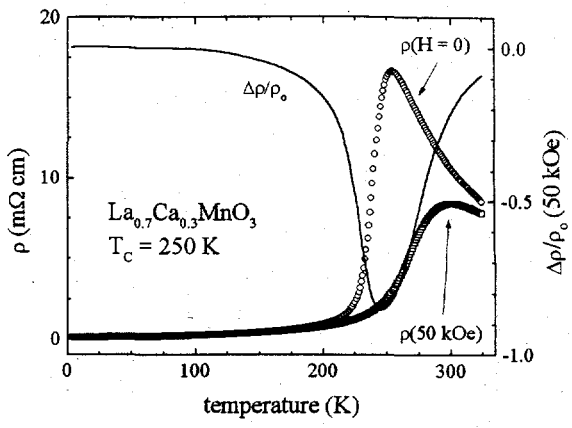

Fig. 2. ρ(T) in H = 0 and 50 kOe (left axis) and transverse MR(T) in 50 kOe (right axis).

50 kOe applied H-field drastically suppresses the peak in ρ at T_C: $\Delta\rho/\rho_o$(50 kOe) = -85% at T_C. Below $T_C/2$ the MR is essentially zero. Measurements on annealed films with T_C's ranging from 150 to 350 K confirm the previous observations [5,6,12,13] that both the resistivity and the MR peak at T_C. Further, for a given field strength, $\Delta\rho/\rho_o(T_C)$ is generally larger for samples with smaller transition temperatures (see below). For example, a specimen with T_C = 150 K displays a -99.6% MR in 50 kOe. For comparison, Jin, *et al.* [12] report a -99.92% MR in a $T_C \approx$ 80 K film at 60 kOe.

The field-dependent resistivity of the T_C = 250 K $La_{0.7}Ca_{0.3}MnO_3$ film is displayed in Fig. 3. Below 100 K the negative MR is extremely small (-0.7% at 100 K in 50 kOe). The data in Fig. 3 show that the MR grows as T increases, reaching its largest saturation values near T_C; the field sensitivity FS ≡ (1/ρ)(dρ/dH) is a maximum just below T_C (FS_{max}(240 K) = -9x10^{-5} Oe^{-1} at 4 kOe, FS_{max}(250 K) = -6x10^{-5} Oe^{-1} at 13 kOe). Despite the very large MR near T_C in 50 kOe, the low-field MR is very small ($\Delta\rho/\rho_o$ at 240 K is -1.6% and -0.02% in fields of 1 kOe and 100 Oe, respectively). ρ(H) does not exhibit cusp-like behavior (a discontinuous dρ/dH at H = 0) at any temperatures; fine-scale measurements near H = 0 reveal that ρ varies as H^2 for H < 2 kOe. Above T_C the MR rapidly drops with increasing temperature.

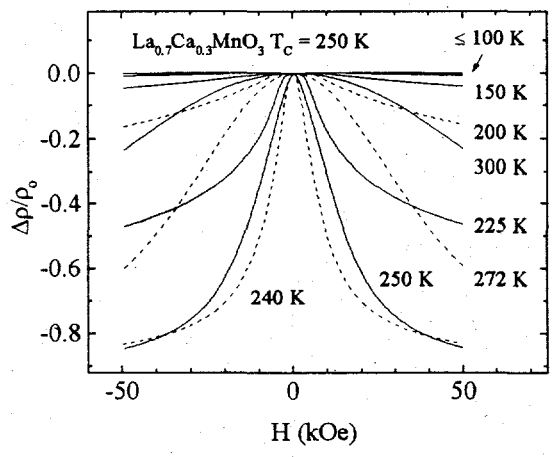

Fig. 3. Transverse MR(H) at number of temperatures from T<100 K to 300 K.

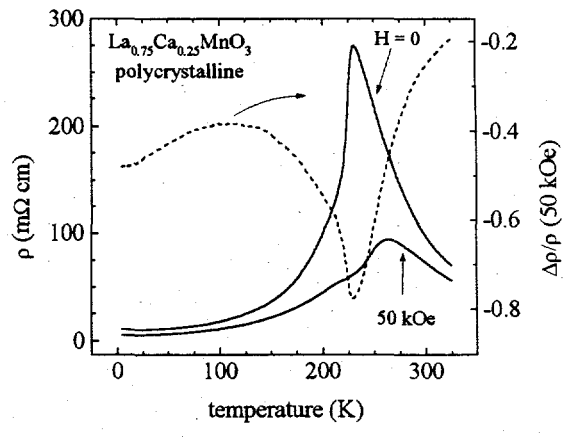

Fig. 4. Ca-doped Polycrystal ρ(T) in H = 0 and 50 kOe (left axis) and transverse MR(T) in 50 kOe (right axis).

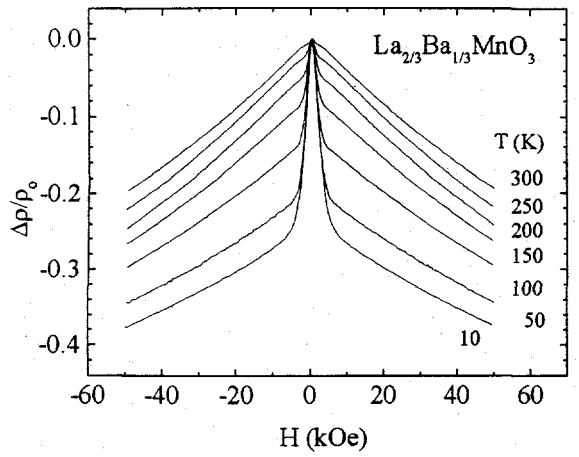

Fig. 5. Transverse MR(H) of a Ba-doped polycrystal at temperatures from 10 to 300 K.

There are important qualitative differences between the temperature-dependent magnetoresistance of thin film and bulk polycrystalline samples. These differences are clearly evident when comparing $\rho(H,T)$ data for a 33% Ca-doped polycrystalline sample (Figs. 4 and 5; $T_C \approx 225$ K) with that of a thin film specimen (Figs. 2 and 3). The zero-field resistivity of the polycrystalline bulk sample exhibits the same overall temperature dependence as the film. In general the MR effect is similar as well, displaying the largest effect at temperatures centered about T_C. The key difference occurs at temperatures well below T_C; while epitaxial films and single crystals [16] display essentially zero MR at low temperatures, polycrystalline samples display a very significant MR effect ($\Delta\rho/\rho_o \approx -0.4$) well below T_C. This difference is a manifestation of the dissimilarities in $\rho(H)$ for films and polycrystalline samples. $\rho(H)$ data for a 33% Ba-doped polycrystal specimen (Fig. 5; $T_C \approx 350$ K) indicate that there is an additional low-field MR effect in polycrystalline samples that is not present in epitaxial specimens. This strongly H-dependent low-field effect is responsible for most of the MR at low temperatures, while its contribution is essentially nonexistent near T_C. This strongly field-sensitive low-temperature MR contribution has been attributed to intergranular charge-transport effects that do not occur in bulk crystalline samples or epitaxial thin films [17].

Transport-Magnetism correlations in CMR films

Figures 1, 2 and 3 indicate that both $d\rho/dH$ and $d\rho/dT$ are largest in the vicinity of T_C; this is precisely the region where dM/dT is a maximum and where an applied H-field could have the greatest effect on the microscopic magnetism. Clearly, there is a close interrelationship between ordered magnetism and charge transport in the manganite CMR compounds. To explore the relationship between $\rho(T)$ and M(T), these quantities are plotted in Fig. 6 for the same thin-film specimen considered in Figs. 1-3. Note that the ρ data are plotted on a log_{10} axis while the M data are plotted on an *inverted* linear axis. The 2 kOe and 10 kOe magnetization data closely follow $\rho(H = 0)$, while M(50 kOe) closely tracks ρ(50 kOe). The low-field (2 kOe) M data do not track $\rho(H = 0)$ below 100 K, which is precisely the temperature range where there is a large difference between M(2 kOe) and M(10 kOe). Bulk magnetization measurements depend on both the local ordered moment and the FM domain structure. M(H) curves at T < 200 K (not shown) are strongly field-

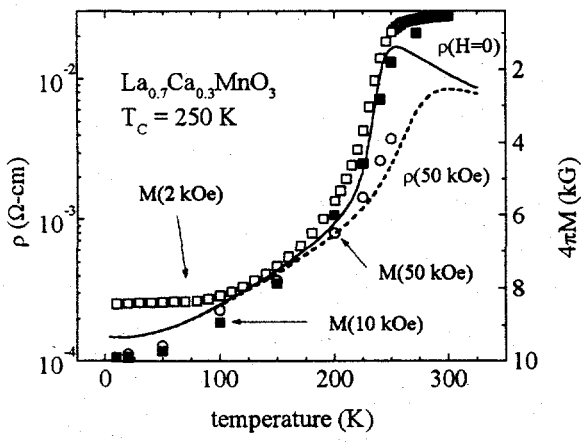

Fig. 6. $\rho(T)$ in H = 0 (solid line) and 50 kOe (dashed line) along the left axis, and M(T) in H = 2 kOe (❑), 10 kOe (■), and 50 kOe (○) along the right axis. M data are plotted on an inverted linear scale.

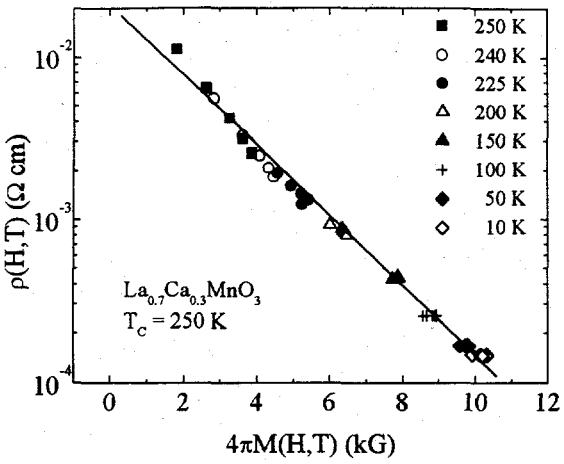

Fig. 7. ρ(H,T) and M(H,T). At each T, points are included at H = 10, 20, 30, 40, and 50 kOe, which progress, respectively, from low to high M values. The solid line is a least-squares fit to the data.

dependent below a characteristic field H_o = 5 kOe. This suggests that M is governed by local magnetism above H_o, while M is determined by the evolving FM domain structure below H_o. The data in Fig. 6 therefore suggest that $ln(\rho)$ follows -M(T) in fields sufficient to make the observed bulk magnetization reflect the local magnetic order.

To more fully examine the ρ-M correlation hinted at by Fig. 6, careful measurements of ρ(H,T) and M(H,T) were made; the results are presented in Fig. 7 where ρ(H,T) is plotted versus M(H,T) rather than as a function of H or T. The data were measured at nine temperatures from 272 K to 10 K in fields sufficient to saturate the domain structure (i.e., at $H > H_o$). The data display a correlation encompassing a two orders of magnitude variation in ρ that can be parameterized as

$$\rho(H,T) = \rho_m \exp\{-M(H,T)/M_o\} \quad . \tag{1}$$

The least-squares fit shown in Fig. 7 gives $\rho_m = 21 \pm 3$ mΩ-cm and $4\pi M_o = 2.02 \pm 0.02$ kG. For temperatures above T_C where FM fluctuations are not observed (at T > 280 K the film is purely paramagnetic, i.e. M∝H) ρ and M are no longer related by Eqn. 1; instead, the resistivity varies as M^2. The nature of the fit in Fig. 7 suggests that the complex T- and H-field dependent transport in $La_{1-x}A_xMnO_3$ is controlled by the underlying magnetization that develops *near* and below T_C.

This resistivity-magnetism correlation was first observed in the manganites by Hundley *et al.* [9] and it has since been confirmed [14,18] by a number of other research groups on thin film samples. Muon spin resonance measurements also detect this relationship between the local zero field magnetization and the resistivity in bulk samples [10]. These bulk measurements indicate that the ρ-M correlation is not a thin-film artifact, but instead is a manifestation of the physical mechanism responsible for the CMR effect in the manganites. Because the correlation is universal and holds throughout the temperature range below T_C it is clear that the CMR compounds are not conventional ferromagnetic metals even well below T_C and that electronic transport is influenced by magnetic order in a highly unconventional manner.

The phenomenology expressed by Eqn. 1 provides important insight into the transport mechanism in the ordered regime. There is no clear theoretical framework that fully describes the

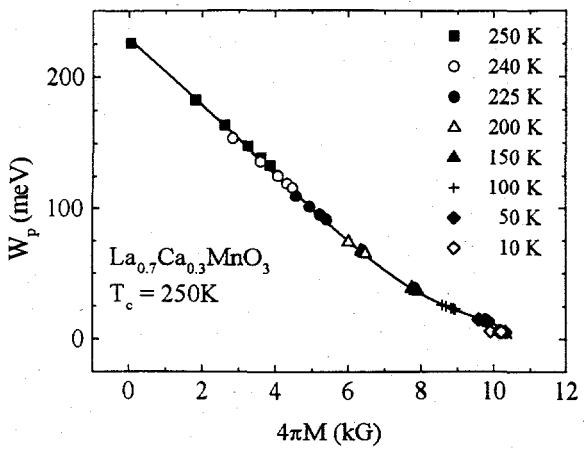

Fig. 8. $W_P(M)$ as calculated from Eqns. 3 and 4 and M(H,T) data presented in Fig. 7. The solid line shows $W_P(M)$ as calculated via Eqns. 3 and 6.

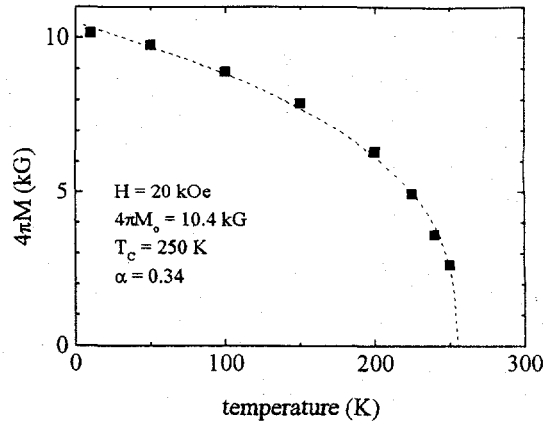

Fig. 9. M(T) data. The dashed line is a fit to the data with Eqn. 5. The fitting parameters are indicated in the figure.

transport state below T_C, making it difficult to determine meaning of this ρ-M correlation. One approach is to assume that the adiabatic small polaron hopping description that is valid above T_C will still apply over a limited temperature range below the ordering temperature. The resistivity of an adiabatic small polaron system is given by [19]

$$\rho = \rho_o T \exp(E_\rho / k_B T) \quad , \tag{2}$$

where ρ_o is a constant, and k_B is Boltzmann's constant. The resistivity activation energy E_ρ is related to the binding energy of an adiabatic polaron W_P (a measure of the degree to which charge carriers are localized) by [19]

$$E_\rho = \frac{W_P}{2} - J + E_o \quad , \tag{3}$$

where E_o is the carrier concentration activation energy as determined from the thermopower (those measurements indicate E_o = 10 meV for 30% Ca-doped manganite films [14]) and J is the bandwidth; for polaronic systems the bandwidth is considerably smaller than the binding energy (we assume $J = W_P/10$).

In order to determine the effect magnetic order has on the polaronic charge carriers we seek a relationship between W_P and M. An expression for E_ρ is realized by equating Eqns. 1 and 2,

$$E_\rho = k_B T \left[\ln\left(\frac{\rho_m}{\rho_o T}\right) - \frac{M}{M_o} \right] \quad . \tag{4}$$

By employing the M(H,T) data displayed in Fig. 7, Eqns. 3 and 4 allow a determination of $W_P(M)$. The resulting binding energy-magnetization relationship is presented in Fig. 8. The $W_P(M)$ plot yields the surprisingly simple result that the binding energy linearly decreases with increasing magnetization. This relationship holds from the onset of magnetic order down to 150 K; this is the temperature where a polaron description is no longer valid because W_P is less than the phonon energy of 40 meV [20]. A clearer understanding of this W_P-M correlation can be

obtained by eliminating temperature in Eqn. 4. The M(T) data depicted in Fig. 9 are well described by the expression

$$M(T) = M_a\left(1-\frac{T}{T_C}\right)^{\alpha} \quad , \tag{5}$$

with $\alpha \approx 1/3$; this exponent is characteristic of a 3d Heisenberg ferromagnet. By inverting this expression, temperature can be eliminated from Eqn. 4 and the resistivity activation energy becomes

$$E_\rho = k_B T_C\left(a - \frac{M}{M_o}+(1-a)\left(\frac{M}{M_a}\right)^3+\frac{M^4}{M_o M_a^3}+O\left[\left(M/M_a\right)^6\right]\right) \quad , \tag{6}$$

where $a \equiv ln(\rho_m/\rho_o T)$. W_P as calculated with Eqn. 6 is included in Fig. 8 as the solid line running through the data points. This expression makes it clear why W_P varies linearly with M: the third-order term only becomes non-negligible when M is a large fraction of M_a.

The linear relationship between polaron binding energy and magnetization indicates that the ρ-M correlation is simply a manifestation of the fact that below T_C the developing magnetic order acts to gradually delocalize the charge-carrier quasiparticles. This delocalization can be brought about by either reducing the temperature or by applying a magnetic field. In either case M(H,T) controls the transport process. The picture that emerges is that of localized small polaron transport at high-T/low-H that evolves into delocalized large polaron transport at low-T/high-H. Small polarons are highly resistive whereas large polarons compounds [21] can exhibit resistivities comparable to poor metals (~100 μΩ cm). The CMR effect comes about from this order-induced carrier delocalization process, an M(H,T)-controlled process that has a profound effect upon the resistivity.

CMR T_C dependence

To determine the dependence of the CMR effect on T_C, we examine the temperature- and H-field dependent resistivity ρ(H,T) of a series of $La_{0.7}A_{0.3}MnO_{3+\delta}$ thin-films (A = Ba, Ca, and Sr) with T_C's ranging from 150 K to 350 K. Both the zero-field resistivity and the magnetoresistance are strongly dependent upon a given film's ordering temperature; low-T_C films exhibit a substantial negative MR, while films with T_C's above 300 K exhibit a more modest MR ratio.

Transport and magnetism measurements were performed on a series of six $La_{0.7}A_{0.3}MnO_{3+\delta}$ thin films grown via pulsed-laser deposition (PLD). The highly oriented, 1000 Å-thick films were deposited on (100) $LaAlO_3$ substrates in a 200 mTorr oxygen atmosphere. The films were post-annealed in flowing oxygen at 950 °C for ten hours. Sample T_C was controlled both by varying the dopant element A [1], and by varying the substrate temperature T_S used during the deposition process. Growth parameters for each film, along with their respective magnetic ordering temperatures (determined from magnetization Arrott plots), are presented in Table I. The Ca-doped films (films 1-4) have T_C's ranging from 150 K to 290 K, while the Ba and Sr-doped films (films 5 and 6) have T_C's that are above room temperature. Both the FM transition width and the low temperature saturation magnetization are T_S-independent. Details of the underlying sample-to-sample differences (stoichiometry, microstructure, etc.) that are responsible for the variation in

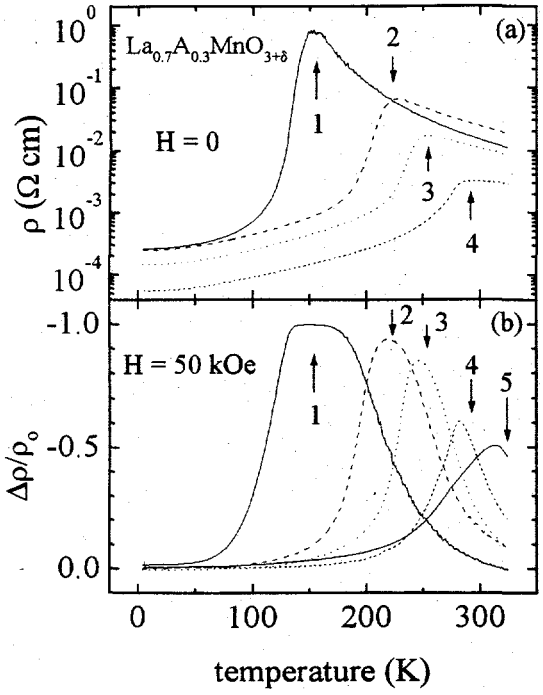

Fig. 10. (a) Resistivity vs. temperature, and (b) 50 kOe MR vs. temperature. The arrows indicate T_C for each sample while the integers indicate the sample number that corresponds to each curve.

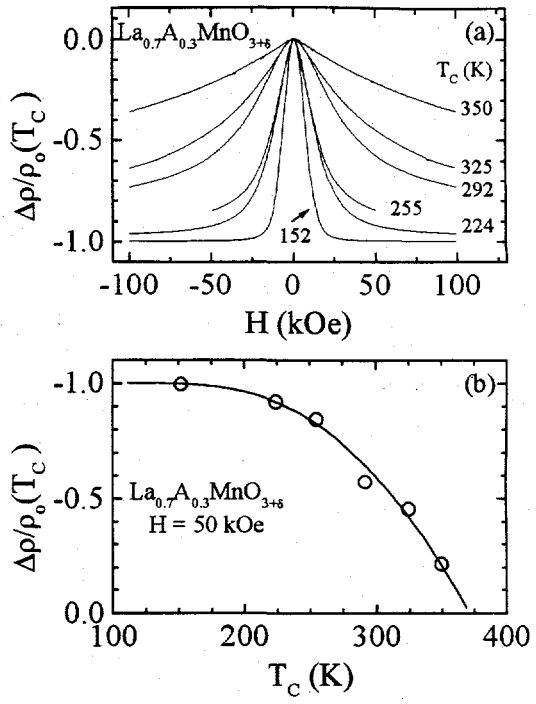

Fig. 11. (a) MR vs. applied field measured at T_C for six samples (T_C for each curve is as indicated). (b) 50 kOe MR measured at T_C for samples 1-6 plotted against sample T_C; the solid line is a fit to the data (see text).

T_C in the Ca-doped samples will not be considered here; the variation is most likely due to T_S-dependent differences in excess oxygen content [13].

The H = 0 resistivities of the films with $T_C < 300$ K are depicted in Fig. 10a. Sample 1 (T_C = 152 K) exhibits a sharp drop in ρ below T_C [$\rho(4K)/\rho(T_C) = 5x10^{-4}$] and activated behavior (activation energy $E_\rho \approx 0.1$ eV) above T_C. Samples 2 and 3 also exhibit activated behavior above T_C with similar E_ρ values. For the other samples, $\rho(T_C)$ progressively decreases with increasing T_C. Well below T_C, ρ saturates to a value near 100 μΩ-cm for all samples. When normalized by their respective low-T resistivities, $\rho(T > T_C)$ roughly fall on a common curve for all samples.

The T-dependent magnetoresistance MR(T) in 50 kOe is shown in Fig. 10b. Sample 1 displays a wide, flat-topped peak centered at T_C with a maximum MR of $\Delta\rho/\rho_o$ = -0.996. With increasing T_C the MR data indicate the following trends: (a) the width of the MR peak decreases, (b) the MR peak temperature T_{max} shifts somewhat below T_C, (c) the magnitude of the MR peak decreases, and (d) $\Delta\rho/\rho_o$ is very small at $T << T_C$ for all six films. MR(T) data measured in H < 50 kOe indicate that T_{max} approaches T_C as H is increased. The H-dependent magnetoresistance MR(H) for samples 1-6 at their

TABLE I. Stoichiometry, substrate temperature T_S, and magnetic ordering temperature T_C for the six $La_{1-x}A_xMnO_{3+\delta}$ thin-film specimens considered here. All films were identically post-annealed.

Sample Number	A	x	T_S (°C)	T_C (K)
1	Ca	0.3	900	152
2	Ca	0.3	750	224
3	Ca	0.3	600	255
4	Ca	0.3	500	292
5	Ba	0.3	600	325
6	Sr	0.3	600	350

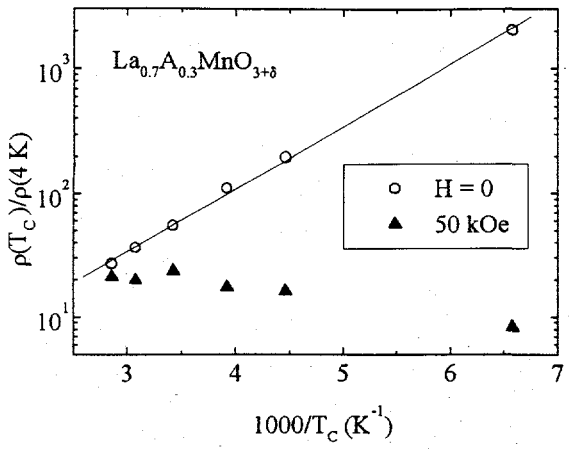

Fig. 12. Normalized resistivity plotted against $1000/T_C$ for samples 1-6 at their respective ordering temperatures in both zero field and 50 kOe.

respective ordering temperatures are shown in Fig. 11a in fields to 100 kOe. Sample 1's MR saturates at a value near $\Delta\rho/\rho_o$ = -1 in 25 kOe; sample 2's MR also saturates, but in a larger H-field and at a smaller value of $\Delta\rho/\rho_o$. The magnetoresistance of samples 3-6 do not saturate even in the largest fields applied. Extrapolations of the MR data to H > 100 kOe for these higher-T_C films suggests that the saturation values of $\Delta\rho/\rho_o$ decreases with increasing T_C.

The key finding from the MR(T,H) data presented in Figs. 10 and 11 is that the size of the CMR effect decreases with increasing film T_C. This result is summarized in Fig. 11b where $\Delta\rho/\rho_o$(50 kOe) at T_C is plotted against sample T_C for films 1-6. The 50 kOe field essentially saturates the MR of sample 1 (T_C = 152 K), reduces ρ by 50% for the film with a T_C near room temperature, and only reduces ρ by roughly 20% for the high-T_C Sr-doped film (film 6). This CMR T_C dependence is simply a reflection of the fact that the order-induced drop in ρ that occurs below T_C is far larger in low-T_C samples than in high-T_C samples. This is made clear in Fig. 12, where $\rho(T_C)$ in both zero field and 50 kOe is plotted versus $1000/T_C$ for the six films; the resistivity is normalized by the low-temperature (4 K) saturation resistivity. The quantity $\rho(T_C)/\rho(4\ K)$ is a measure of the reduction in ρ brought on by complete FM order. In zero-field $\rho(T_C)/\rho(4\ K)$ varies as $\exp(E_\rho/T_C)$ with an activation energy E_ρ = 0.1 eV. This is the same activation energy evident in $\rho(T > T_C)$ in films 1-3. The normalized resistivity in 50 kOe is essentially T_C-independent. The zero-field and 50 kOe results in Fig. 12 lead directly to the expression

$$\Delta\rho/\rho_o = \beta\exp(-E_\rho/T_C) - 1 \qquad (7)$$

that is displayed in Fig. 11b (with β = 20). The data in Figs. 11b and 12 indicate that the key quantity that controls the MR in a given film is the normalized resistivity $\rho(T_C)/\rho(4\ K)$ (which is set by T_C), and not just $\rho(T_C)$. Hence, attempts to increase $\rho(T_C)$ by growth non-optimization should also increase $\rho(4\ K)$, and would presumably have little affect on the magnitude of the CMR effect.

CONCLUSIONS

The characteristic H-field strength sufficient to substantially reduce ρ provides insight into the charge-carrier's nature. In a single-electron description the characteristic field H_{eff} required to affect ρ by influencing the magnetic order is roughly given by $gS\mu_B H_{eff} \approx k_B T_C$. With $g = 2$, $S = 1.85$ (valid for $x = 0.3$), and $T_C = 250$ K, we find $H_{eff} \approx 1$ MOe, 100 times larger then the 10 kOe field required to significantly reduce ρ experimentally. This indicates that an energy scale far smaller than the FM exchange energy ($J \approx k_B T_C$) characterizes the conduction process in these compounds. The effective energy scale is quite small ($E_{eff} \approx 58$ μeV (0.7 K) for $H_{eff} \approx 10$ kOe), and it presumably characterizes the magnetic polaron. The rapid rate at which the polaron binding energy is reduced by the order-induced magnetization indicated in Fig. 8 ($dW_P/dM \approx 20$meV/kG) also indicates that the polaron is destroyed at a rate far above what would be expected on simple energy scale arguments. While there is clear local-structure [22] and transport evidence [14,15] for the existence of the small polarons above T_C, the challenge is to extend our theoretical understanding of the underlying physics that describes the interplay between magnetic order and polaronic quasiparticles in the CMR manganites.

The strong H-field and T dependencies of ρ appear to be dictated by the local magnetism in $La_{0.7}Ca_{0.3}MnO_3$. The nature of the $\rho(H,T)$-$M(H,T)$ correlation suggests that below T_C the conduction process involves quasiparticle hopping. The considerable H and T dependence of ρ in the doped lanthanum-manganates indicates that the nature of the quasiparticle must be qualitatively altered by the application of an H-field or by a reduction in temperature. It appears that the magnetization that develops as a result of magnetic order acts to delocalize the trapped polaronic carriers by progressively reducing the electron-phonon binding energy W_P.

The field-dependent resistivity measurements on a series of six PLD-grown CMR films indicate that the magnitude of the CMR effect is determined by a given film's magnetic ordering temperature. Films with a low T_C exhibit both a large drop in the resistivity in the FM state and a large, negative magnetoresistance, while both effects are significantly smaller in films with a high ordering temperature.

ACKNOWLEDGMENTS

The authors thank S. Billinge, D. Emin, F. Garzon, M. Hawley, G. Kwei, J. Tesmer, and H. Röder for informative discussions and encouragement. This work was performed under the auspices of the U.S. Department of Energy.

REFERENCES

* Present address: department of Physics, Florida Atlantic University, Boca Raton, Florida 33431.

1. G.H. Jonker and J.H. Van Santen, Physica **16**, 337 (1950); **16**, 599 (1950).

2. E.O. Wollan and W.C. Koehler, Phys. Rev. **100**, 545 (1955).

3. J. Volger, Physica **20**, 49 (1954).

4. C. Zener, Phys. Rev. **82**, 403 (1951); P.W. Anderson and H. Hasegawa, Phys. Rev. **100**, 675 (1955); P.G. deGennes, Phys. Rev. **118**, 1412 (1960).

5. R.M. Kusters, J. Singleton, D.A. Keen, R. McGreevy, and W. Hayes, Physica B **155**, 362 (1989); K. Chahara, T. Ohno, M. Kasai, and Y. Kozono, Appl. Phys. Lett. **63**, 1990 (1993).

6. R. von Helmolt, J. Wecker, B. Holzapfel, L. Schultz, and K. Samwer, Phys. Rev. Lett. **71**, 2331 (1993).

7. A.J. Millis, P.B. Littlewood, and B.I. Shraiman, Phys. Rev. Lett. **75**, 5144 (1995).

8. H. Röder, J. Zang, and A.R. Bishop, Phys. Rev. Lett. **76**, 1356 (1996); A.J. Millis, Phys. Rev. B **53**, 8434 (1996); D. Emin, M.S. Hillery, and Nih Liu Phys. Rev. B **35**, 641 (1987).

9. M.F. Hundley, M. Hawley, R.H. Heffner, Q.X. Jia, J.J. Neumeier, J. Tesmer, J.D. Thompson, and X.D. Wu, Appl. Phys. Lett. **67**, 860 (1995).

10. R.H. Heffner, L.P. Le, M.F. Hundley, J.J. Neumeier, G.M. Luke, K. Kojima, B. Nachumi, Y.J. Uemura, D.E. MacLaughlin, and S.W. Cheong, Phys. Rev. Lett. 77, 1869 (1996).

11. M.F. Hundley, J.J. Neumeier, R.H. Heffner, Q.X. Jia, X.D. Wu, and J.D. Thompson, J. Appl. Phys. **79**, 4535 (1996).

12. S. Jin, T.H. Tiefel, M. McCormack, R.A. Fastnacht, R. Ramesh, and L.H. Chen, Science **264**, 413 (1994).

13. H.L. Ju, C. Kwon, Q. Li, R.L. Greene, and T. Venkatesan, Appl. Phys. Lett. **65**, 108 (1994).

14. M. Jamie, M.B. Salamon, M. Rubinstein, R.E. Treece, J.S. Horwitz, and D.B. Chrisey, Phys. Rev. B **54**, 11914 (1996).

15. M. Jaime, H.T. Hardner, M.B. Salamon, M. Rubinstein, P. Dorsey, and D. Emin, Phys. Rev. Lett. **78**, 951 (1997); M.F. Hundley and J.J. Neumeier, Phys. Rev. B (in press).

16. V.H. Crespi, L. Lu, Y.X. Jia, K. Khazeni, A. Zettl, and M.L. Cohen, Phys. Rev. B **53**, 14303 (1996).

17. H.L. Ju, J. Gopalakrishnan, J.L. Peng, Qi Li, G.C. Xiong, T. Venkatesan, and R.L. Greene, Phys. Rev. B **51**, 6143 (1995); H.Y. Hwang, S-W. Cheong, N.P. Ong, and B. Batlogg, Phys. Rev. Lett. 77, 2041 (1996).

18. J.Z. Sun, L. Krusin-Elbaum, S.S.P. Parkin, and Gang Xiao, Appl. Phys. Lett. **67**, 2726 (1995); B.X. Chen, C. Uher, D.T. Morelli, J.V. Mantese, A.M. Mance, and A.L. Micheli, Phys. Rev. B **53**, 5094 (1996); B. Martinez, J. Fontcuberta, A. Seffar, J.L. Garciamunoz, S. Pinol, and X. Obradors, Phys. Rev. B ***54***, 10001 (1996).

19. I.G. Austin and N.F. Mott, Adv. Phys. **18**, 41 (1969); N.F. Mott and E.A. Davis, *Electronic Processes in Noncrystalline Materials* (Oxford, Clarendon Press, 1979); D. Emin, *Electronic and Structural Properties of Amorphous Semiconductors*, edited by P.G. Le Comber and J. Mort (Academic Press, London, 1973) p. 261.

20. Y. Okimoto, T. Katsufuji, T. Ishikawa, A. Urushibara, T. Arima, and Y. Tokura, Phys. Rev. Lett. **75**, 109 (1995).

21. T. Kasuya, A. Yanase, and T. Takeda, Solid State Commun. **8**, 1551 (1970); D. Emin, Phys. Rev. B **48**, 13691 (1993).

22. S.J.L Billinge, R.G. Difrancesco, G.H. Kwei, J.J. Neumeier, and J.D. Thompson, Phys. Rev. Lett. **77**, 715 (1996).